

NOTE

Study of the NEMCA Effect in a Single-Pellet Catalytic Reactor

It has been recently found (1–15) that solid electrolytes can be used as active catalyst supports to dramatically alter the catalytic properties of porous metal catalyst films by polarizing the metal–solid electrolyte interface. This new effect of non-Faradaic electrochemical modification of catalytic activity (NEMCA) has been demonstrated using both O^{2-} and Na^+ conducting solid electrolytes. It has been attributed to the controlled change in catalyst work function and to the concomitant changes in the strength of chemisorptive bonds due to ion spillover onto the catalyst surface created at the three-phase boundaries upon polarization of the metal–solid electrolyte interface (1, 2, 4–10). NEMCA can induce reversible catalytic rate changes up to 7000% with significant changes in product selectivity (1–15). The increase in catalytic rate can be up to a factor of 3×10^5 higher than the rate of ion transfer to or from the catalyst film (2, 5).

In all previous NEMCA studies (1–15) the counter and reference electrodes were exposed to ambient air, being deposited on the outer side of the bottom of a solid electrolyte tube opposite to the catalyst-working electrode, which was deposited on the bottom in the inner side of the tube where the catalytic reaction was taking place (Fig. 1a).

This electrode configuration is similar to the one used in fuel cells and although it offers some specific advantages, like a constant gas composition over the reference electrode, it suffers from the lack of easy applicability in conventional flow reactors, where the electrodes–solid electrolyte system has to be surrounded by the flowing

gas mixture. Such an arrangement, albeit without a reference electrode, has been already used successfully during CH_4 oxidation on catalyst films deposited on YbSr CeO_3 (16, 17) or yttria-stabilized zirconia (17–19) using a two electrode configuration. In these cases rate changes as high as 800% were observed, but due to the high operating temperatures ($T > 700^\circ C$) these rate increases were Faradaic, i.e., the catalytic rate changes were almost equal to the rate of ion transfer through the solid electrolyte.

In this work we examine the possibility of inducing NEMCA during C_2H_4 oxidation on Pt utilizing a stabilized ZrO_2 pellet with both sides exposed to a reacting C_2H_4/O_2 mixture so that all three electrodes (catalyst, counter, and reference) are exposed to the reacting mixture. This reaction has been recently investigated in a fuel-cell type reactor and found to exhibit a pronounced NEMCA effect (5). Furthermore, we examine the existence of differences in NEMCA behaviour for different arrangements of the counter and reference electrodes relative to the catalyst-working electrode.

The continuous flow atmospheric pressure CSTR-type reactor used in this study is shown schematically in Fig. 1b. The ZrO_2 (8 mol% Y_2O_3) (YSZ) dense pellet used had a diameter of 3/4" and a thickness of 3 mm. The catalyst-working electrode was a porous platinum film deposited on the stabilized zirconia pellet using thin coatings of A1121 Engelhard platinum paste followed by calcining first at $400^\circ C$ for 2 h and then at $840^\circ C$ for 20 min. The zirconia pellet (disc) was suspended in a quartz tube as shown in Fig. 1b. Pt wires attached to the catalyst and

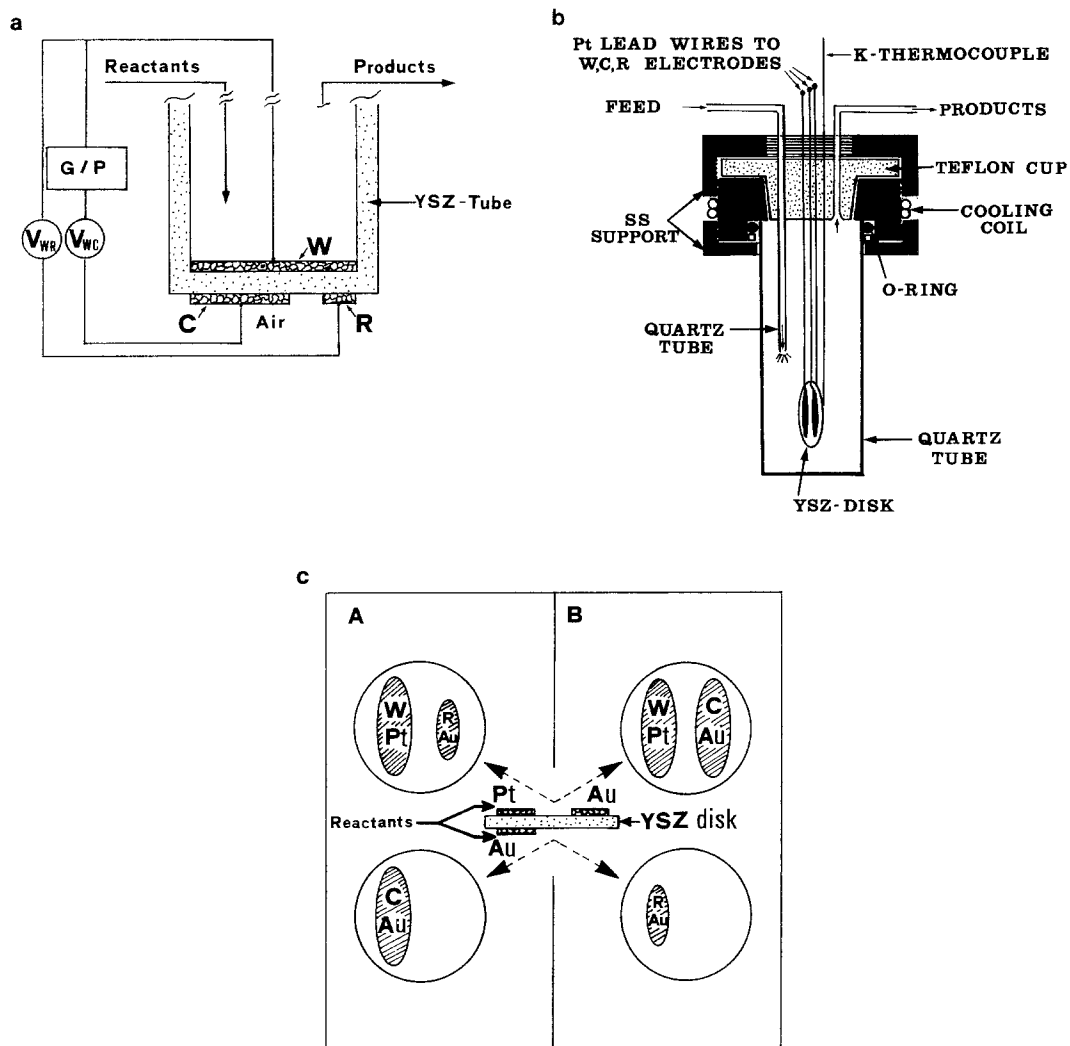


FIG. 1. Catalyst (W), counter (C) and reference (R) electrodes configuration in previous NEMCA studies (a), and reactor (b) and electrodes configuration (c) in the present study; G/P: galvanostat-potentiostat.

to the counter and reference electrodes were fed into the quartz reactor through an appropriately machined Teflon component which was screwed into the water-cooled stainless steel reactor cap. The porous counter and reference electrodes were made of gold, which for the conditions used here was found to be practically inert for the catalytic reaction under consideration. They were deposited on the stabilized zirconia pellet by application of thin coatings of M8032 Deme-

tron gold paste. The calcining procedure was the same as the one for the working electrode. The superficial catalyst surface area was 1 cm^2 . The true catalyst surface area was measured by surface titration of oxygen with C_2H_4 as described in detail elsewhere (2). The measured surface area value was 11 cm^2 , corresponding to a reactive oxygen catalyst uptake $N = 2.72 \cdot 10^{-8}$ g-atom O.

Two electrode configurations were used

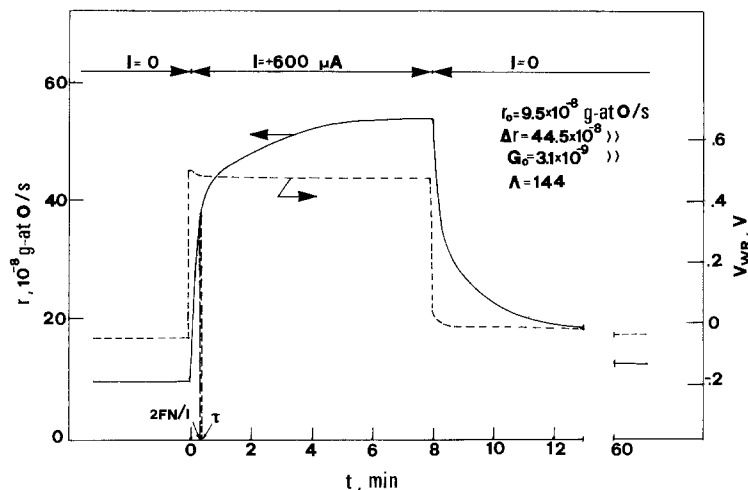


FIG. 2. Rate and catalyst potential response to step change in applied current during C_2H_4 oxidation on Pt. Comparison of experimental (τ) and computed ($2FN/I$) relaxation time constants; $T = 510^\circ C$, $P_{O_2} = 14 \times 10^{-2}$ bar, $P_{C_2H_4} = 6.7 \times 10^{-3}$ bar, total molar flow rate $G = 5.7 \times 10^{-3}$ mole/s. Configuration A.

(Fig. 1c). In configuration A the working (W) and reference (R) electrodes are deposited on the same side of the pellet and the counter (C) electrode is deposited on the other side, opposite to the catalyst-working electrode. Configuration B corresponds to interchanging the positions of counter and reference electrodes in configuration A. As described in previous works (2, 5, 6), this three-electrode system allows for accurate measurement of catalyst overpotential and catalyst-solid electrolyte exchange current I_0 .

The gas feed and product analysis unit utilizing on-line gas chromatography, mass spectrometry, and IR spectroscopy has been described previously (2-10), along with electrode preparation and characterization details. Reactants were L' Air Liquide certified standards of 21% O_2 in He and 10% C_2H_4 in He, and could be further diluted by using ultrapure He.

Figure 2 shows a typical galvanostatic transient, i.e., a typical catalytic rate transient when a constant current I , and thus a constant flux of O^{2-} equal to $I/2F$, is supplied to the catalyst. This transient corre-

sponds to configuration A, but the behaviour is exactly the same also for configuration B. At the start of the experiment the circuit is open and the catalyst is at steady-state activity, corresponding to a reaction rate $r_0 = 9.54 \times 10^{-8}$ g-atom O/s. At time $t = 0$, a galvanostat is used to apply a constant current $I = +600 \mu A$ with a corresponding rate of oxygen transfer $G_0 = I/2F = 0.31 \times 10^{-8}$ g-atom O/s. This causes an approximately sixfold increase in the rate of C_2H_4 oxidation to CO_2 and H_2O . The rate increase $\Delta r = 44.5 \times 10^{-8}$ g-atom O/s is a factor of 144 greater than G_0 , i.e., the reaction exhibits the NEMCA effect with an enhancement factor $\Lambda = \Delta r/G_0$ equal to 144. This implies that each O^{2-} supplied to the catalyst causes 144 chemisorbed oxygen atoms to react with C_2H_4 and produce CO_2 and H_2O . At the same time the voltage difference between the catalyst and the reference electrode changes from -20 mV to a steady-state value of $+480$ mV. Upon opening the circuit the catalytic rate and catalyst potential are restored to their initial values within 50 min. The above transient behaviour is similar to the one for the case of

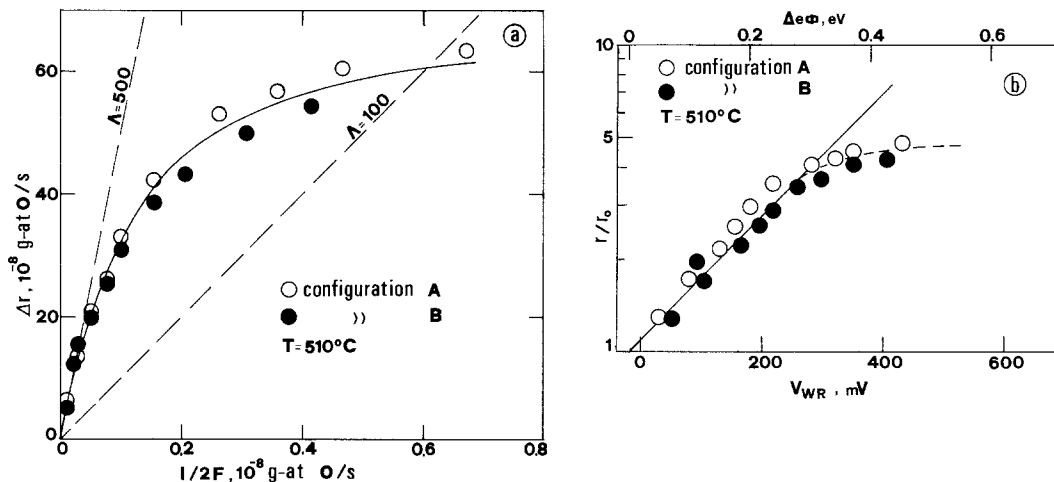


FIG. 3. Steady-state effect of applied current on the rate of C_2H_4 oxidation (broken lines are constant enhancement factor lines) (a) and effect of catalyst potential V_{WR} and corresponding work function change $\Delta(e\Phi)$ on the rate of C_2H_4 oxidation (b). Conditions: $P_{\text{O}_2} = 13.6 \times 10^{-2}$ bar, $P_{\text{C}_2\text{H}_4} = 8.0 \times 10^{-3}$ bar, total molar flow rate $G = 5.6 \times 10^{-5}$ mole/s, $r_0 = 1.7 \times 10^{-7}$ g-atom O/s for both electrode configurations A and B.

ambient-air-exposed counter and reference electrodes (5). Here also the rate increase relaxation time constant τ is almost equal to $2FN/I$, where N is the true catalyst surface area, equal to 2.72×10^{-8} g-atom O as measured by a surface titration technique (2, 3, 10). This shows once again that the NEMCA effect is not an electrocatalytic phenomenon, but a catalytic one taking place over the entire catalyst surface.

The steady-state effect of applied current I on the rate of ethylene oxidation, expressed in terms of the rate of atomic oxygen consumption, is presented in Fig. 3a. As shown in the figure, enhancement factor Λ values as high as 500 have been measured. These values are in good agreement with Λ values obtained from the equation $\Lambda \approx 2Fr_0/I_0$, which has been found to successfully predict the order of magnitude of Λ for different catalytic systems (1–15). The value of the exchange current I_0 was determined from Tafel plots and was found equal to $15 \mu\text{A}$. The leveling-off of the curve at high current values is due to changing of the reaction order with respect to C_2H_4 and oxygen, as discussed in detail elsewhere (5).

Figure 3b shows the effect of catalyst potential on the rate enhancement ratio r/r_0 . Up to a certain catalyst potential, where the catalytic rate is first order in C_2H_4 and zeroth order in oxygen (5), there is an exponential increase of ethylene oxidation rate with potential according to the equation

$$\ln(r/r_0) = \alpha F(V_{WR} - V_{WR}^*)/RT, \quad V_{WR} > V_{WR}^*, \quad (1)$$

with $\alpha = 0.35$ and $V_{WR}^* = -20$ mV (F is Faraday's constant).

As shown both theoretically (2, 5) and experimentally (1, 15) using a Kelvin probe, polarization of the catalyst–solid electrolyte interface induces changes in the work function $e\Phi$ of the gas exposed catalyst surface which are due to spillover of oxygen ions, accompanied by their compensating charges in the metal, onto the catalyst surface. The creation of such spillovering species depends on the presence of significant catalyst–electrolyte activation overpotential (2). Under severe polarization conditions the overall electrocatalytic reaction $\text{O}^{2-} \rightarrow \text{O}(a) + 2e^-$ is slow and rate limiting for the

transfer of O^{2-} from the counter electrode to the catalyst, so that partially charged oxygen species can be created at the three phase boundaries, very probably O^- (2, 5). They then diffuse over the entire catalyst surface altering the work function of the gas-exposed (catalytically active) metal surface. The induced work function change, which causes an alteration in the strength of chemisorptive bonds (2, 20) is exactly equal to the change in the ohmic drop free catalyst potential V_{WR} relative to the reference electrode (2, 7, 15). The second abscissa axis in Fig. 3b is constructed on the basis on this equality.

The general result of this investigation is that one can induce NEMCA irrespective of electrode arrangement and gas composition over the counter and reference electrodes. It must be pointed out that although the reference electrode here is not exposed to a reference atmosphere but to the reaction mixture, the general correlations of the NEMCA effect (2, 7, 8) involving V_{WR} are still valid. This is not surprising, as the conversions employed in this study are less than 15%, which in the region of exponential rate increase leaves the gaseous composition over the reference electrode practically unaffected. Comparison of the results for the different electrode configurations employed in this study shows that as soon as a certain overpotential is created at the catalyst–solid electrolyte interface and the catalyst acquires a corresponding ohmic-drop-free potential there is a certain catalytic rate change given by Eq. (1) regardless of the position of counter electrode, i.e., regardless of the macroscopic geometry of the electric field between the working and the counter electrodes. The only difference for different counter electrode arrangements is the magnitude of the ohmic drop between the working and counter electrodes, which in any case is desirable to be kept as low as possible.

The investigation shows that the NEMCA effect can be effectively used to induce catalytic activity enhancement in conventional-

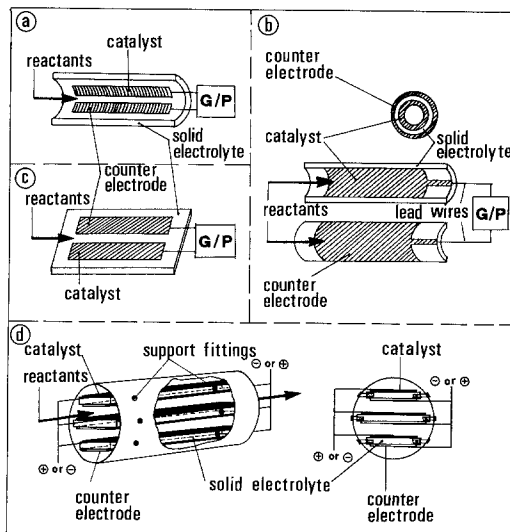


FIG. 4. Possible catalytic reactor designs for NEMCA applications: cylindrical and planar component geometries (a,b,c) and planar sheet–cylindrical reactor configuration (d).

type catalytic reactors, avoiding the complexity of gas-tightness required in fuel-cell-type reactors. A possible reactor design may include the solid electrolyte in the form of a tube or of parallel tubes or of a planar sheet or planar ribbed parallel sheets so that channels between the sheets are formed (21). Some examples of possible designs are presented in Fig. 4. The counter electrode may be deposited on the same side or opposite to the catalyst-working electrode. The only remaining complexity is the need of introduction of conductive wires or metal films to establish electrical contact with the catalyst and counter electrodes in the reactor. Some possibilities for avoiding these practical problems are discussed elsewhere (2, 21).

This investigation shows the feasibility of utilizing the NEMCA effect in systems where not only the catalyst-working electrode but also the counter and reference electrodes are exposed to the reaction mixture, under various arrangements relative to the position of the catalyst.

The results show that solid electrolytes can be used as active catalyst supports and

that the NEMCA effect can be used successfully in conventional-type flow catalytic reactors. This seems very promising from a technological point of view.

ACKNOWLEDGMENTS

We thank Professor C. G. Vayenas for useful discussions. Financial support by the EEC Non-nuclear Energy, JOULE and SCIENCE Programmes is also gratefully acknowledged.

REFERENCES

1. Vayenas, C. G., Bebelis, S., and Ladas, S., *Nature (London)* **343** (6259), 625 (1990).
2. Vayenas, C. G., Bebelis, S., Yentekakis, I. V., and Lintz, H.-G., "Non-Faradaic Electrochemical Modification of Catalytic Activity: A status report," *Catalysis Today*, Vol. 11, No. 3, p. 303. Elsevier, Amsterdam, 1992.
3. Yentekakis, I. V., and Vayenas, C. G., *J. Catal.* **111**, 170 (1988).
4. Vayenas, C. G., Bebelis, S., and Neophytides, S., *J. Phys. Chem.* **92**, 5083 (1988).
5. Bebelis, S., and Vayenas, C. G., *J. Catal.* **118**, 125 (1989).
6. Neophytides, S., and Vayenas, C. G., *J. Catal.* **118**, 147 (1989).
7. Vayenas, C. G., Bebelis, S., Neophytides, S., and Yentekakis, I. V., *Appl. Phys. A* **49**, 95 (1989).
8. Vayenas, C. G., Bebelis, S., Yentekakis, I. V., Tsiakaras, P., and Karasali, H., *Platinum Met. Rev.* **34**(3), 122 (1990).
9. Vayenas, C. G., and Neophytides, S., *J. Catal.* **127**, 645 (1991).
10. Vayenas, C. G., Bebelis, S., and Despotopoulou, M., *J. Catal.* **128**, 415 (1991).
11. Lintz, H.-G., and Vayenas, C. G., *Angew. Chem.* **101**, 725 (1989); *Angew. Chem. Int. Ed. Engl.* **28**, 708 (1989).
12. Vayenas, C. G., Bebelis, S., and Neophytides, S., in "New Developments in Selective Oxidation" (G. Centi and P. Trifiro, Eds.), *Studies in Surface Science and Catalysis*, Vol. 55, p. 643. Elsevier, Amsterdam, 1990.
13. Vayenas, C. G., Bebelis, S., Yentekakis, I. V., Tsiakaras, P., Karasali, H., and Karavasilis, Ch., *ISSI Lett.* **1**, 5 (1991).
14. Vayenas, C. G., Bebelis, S., and Kyriazis, C. C., *Chem. Tech.* **21**, 500 (1991).
15. Ladas, S., Bebelis, S., and Vayenas, C. G., *Surf. Sci.* **251/252**, 1062 (1991).
16. Chiang, P.-H., Eng, D., and Stoukides, M., *J. Electrochem. Soc.* **138**, L11 (1991).
17. Eng, D., and Stoukides, M., *Catal. Rev.-Sci. Eng.* **33**, 375 (1991).
18. Otsuka, K., Suga, K., and Yamanaka, I., *Chem. Lett.*, 317 (1988).
19. Otsuka, K., Suga, K., and Yamanaka, I., *Catal. Lett.* **1**, 423 (1988).
20. Boudart, M., *J. Am. Chem. Soc.* **74**, 3556 (1952).
21. Vayenas, C. G., Bebelis, S., Yentekakis, I. V., and Tsiakaras, P., European Patent Appl. 90600021.1 (1990).

I. V. YENTEKAKIS AND S. BEBELIS

*Institute of Chemical Engineering
& High Temperature Chemical Processes
Department of Chemical Engineering
University of Patras
GR-26110 Patras
Greece*

Received February 4, 1992; revised April 23, 1992